APPENDIX G

GEOSTATISTICAL MODELING FOR THE OU 3 STUDY AREA

GEOSTATISTICAL MODELING FOR THE OU3 STUDY AREA OF THE UPPER COLUMBIA RIVER SITE

RedDot3D Inc.

March 2025

Contents

List of Maps

List of Figures

List of Tables

Abbreviations and Acronyms

C	Observed concentration value
Cd	Cadmium
EPA	Environmental Protection Agency
ERM	Environmental Resources Management
ln	natural logarithm
m	meters
Max	Maximum
Min	Minimum
OU	Operable Unit
p	optimal parameter (λ in technical literature)
P10	10th Percentile
P50	Median
P90	90th Percentile
Pb	Lead
ppm	Part(s) per million
RI	Remedial Investigation
SGS	Sequential Gaussian Simulation
SUB1	Subset I
SUB2	Subset II
T	Transformed Box-Cox value
TAI	Tech American Incorporated
Transf.	Transformation
UCR	Upper Columbia River
UK	Universal Kriging
US	United States
UTM	Universal Transverse Mercator
WA	Washington State
Zn	Zinc

Introduction

This study presents geostatistical modeling of soil metal concentrations in the Operable Unit (OU) 3 study area of the Upper Columbia River site. Geostatistics is a specialized field within applied statistics that models spatially distributed data, providing reliable estimates at unsampled locations and quantifying associated uncertainties.

The text description of Mapping Methodology, Database, Data Analysis, Post-Processing, and Conclusions are presented immediately below, followed by maps, figures and tables. The various maps are shown in Maps 1 - 15, the statistical analysis in Figures 1 - 7, the local coordinate system in Figure 8, and validation checks in Figures 9 - 12.

Mapping Methodology

The geostatistical modeling completed for the Upland Remedial Investigation (RI) has three main objectives:

1) The predictions of lead, cadmium, and zinc concentrations in unsampled surface soil
2) The prediction of the uncertainty in the estimated concentrations, and
3) Preparation of maps showing the probabilities of concentrations exceeding specific concentrations.

Geostatistics offers a toolkit for developing all the maps that are needed: the estimates of soil concentrations, the associated uncertainties, and the probabilities of exceeding specific thresholds. This approach has been used for environmental studies for over 40 years, with some of the earliest applications being surface soil contamination studies conducted using the Geostatistical Environmental Assessment Software (GeoEAS) software by the EPA in the 1980s (Englund and Sparks, 1988).

The specific geostatistical tools used for the UCR studies are: Sequential Gaussian Simulation and Universal Kriging, also known as "kriging with a trend model."

The factors that create uncertainty in predicted concentrations include: laboratory measurement error, distance from nearby samples, the variability of nearby samples and the ability to recognize and model local trends. These will all contribute to uncertainty and cause it to vary spatially across the study area. To support future RI decision-making, the Upland RI will need these spatially varying uncertainties to be predicted, i.e. for each map of surface soil concentrations an associated map of predicted uncertainties. Because there is uncertainty in the estimates at every location, there is also a chance that the true but unknown concentration will exceed thresholds relevant to human health and environmental protection. For future decisions related to possible remedial actions, maps are also needed for the spatially varying probabilities that the unknown soil concentration exceeds specific thresholds.

Sequential Gaussian Simulation (SGS)

SGS (Gómez and Journel, 1993) is a method used to model spatial uncertainty by producing a set of 100 equally probable maps that honor:

- sample data at specific locations
- their distribution (histogram)
- their pattern of spatial variation (variogram)

SGS is often referred to as a "spatial Monte Carlo" method because it implements random sampling of a model spatially. The maps that it produces are all plausible renditions of actual surface soil concentrations. The 100 different simulated values at each location were used to:

- calculate a predicted value: the 50th percentile (P50) by taking the median of the 100 values
- quantify uncertainty: the difference between the 90th percentile (P90) and the 10th percentile (P10)
- calculate probabilities of exceedance: a count of the number of times a simulated value exceeds a given threshold

SGS uses nearby data to estimate the mean and variance of the local distribution, then sequentially samples random values from these Gaussian distributions to create multiple realistic scenarios. The method used to estimate the local means and variances is called "kriging" in geostatistics, which is the same as what is referred to as "Gaussian Process Regression" in other branches of statistics. There are several different types of kriging, which differ in the assumption made about the local mean. The specific kriging approach used for these studies is "universal kriging."

Universal Kriging (UK)

UK (Matheron, 1969) is applied for estimating local probability distributions when local trends are believed to exist. It does not explicitly model large-scale regional data trends; instead, it relies on nearby data to fit a local trend that depends on spatial coordinates. UK effectively captures large-scale data trends indirectly by combining numerous local trends into a coherent regional model. In UK, the user chooses the functional form of the trend (linear, quadratic, cubic, sinusoidal, etc.) and also decides the coordinates along which these functions should be used. As discussed below, linear local trends were used in these geostatistical modeling studies and were a function of local coordinates (X'Y') that are aligned parallel and perpendicular to the Columbia River.

Mapping Area and Grid

Map 1 shows the footprint of the UCR study area within which metal concentrations of surface soils were mapped. The perimeter of this area extends 2,500 m beyond the available samples used for surface soil mapping and is bounded on the northern edge by the US-Canada border. Within this footprint, estimates were calculated at the center of square 30 m cells that are aligned with UTM coordinates. The choice of 2,500 m was made by testing various possible extrapolation distances and choosing the one that created a single contiguous region. At smaller extrapolation distances, the footprint became a collection of separate islands. At larger distances, the outermost estimates depended mostly on the local trend model calculated by UK; the extrapolation of the local trend several kilometers past the last available sample made the outermost estimates unreliable and not useful for sampling decisions and remediation planning.

The estimates for each 30 m cell were based on the closest 30 samples.

Database

The data set utilized for this analysis was the Upland RI Data Set provided as Appendix D to the Revised Draft Final Upland RI Report. The data set was approved by EPA on August 23, 2024, in email correspondence from Bonnie Arthur to Rob Orr.[1]

Samples analyzed in this study were classified into two subsets; Subset I comprises the set of samples used to map metal concentrations (Map 2). Subset II consists of a smaller collection of samples gathered specifically around historical mining and milling areas within the region (Map 3). These two subsets overlap spatially to some extent, i.e. some of the Subset II samples lie within the mapping footprint

[1] USEPA (U.S. Environmental Protection Agency). 2024. Personal communication (email to Rob Orr, TAI, dated August 23, 2024, from Bonnie Arthur, EPA Remedial Project Manager, regarding Proposed Geostatistical Modeling Data Set). U.S. Environmental Protection Agency, Seattle, WA.

defined for Subset I. Analysis of the spatial variation in the two subsets showed that the range of correlation is low for the mines-and-mills data and their short-scale variation is very high (Figure 1)[2].

These two characteristics entail that attempting to predict Subset II concentrations at locations where there are no samples is going to lead to unreliable estimates; for this reason, it is only the surface soil samples in Subset I that were spatially interpolated and mapped. The locations and concentrations of Subset II are displayed spatially, but no attempt has been made to produce grids of predicted values for Subset II.

The data set included 1,406 samples in total. Subset I contained the majority, with 1,106 sample locations with laboratory measurements for Pb and Cd and 875 for Zn; Subset II had 300 samples. Within Subset I, there were 26 samples in British Columbia, Canada, located within 1 km of the US-Canada border. Samples from Canada were included in the mapping of surface soil concentrations because they improved the reliability of estimates just south of the border.

The concentration distributions of Pb, Cd, and Zn in each subset are shown in the histograms in Figures 2, 3, and 4 and Tables 1, 2, and 3.

Data Analysis

Spatial Trends

Geochemical distributions of Pb, Cd, and Zn in the study area exhibit significant statistical spatial trends influenced by distance from-the-river and distance along-the-river. As shown in Figure 5, the range of correlation for Pb along the river is three times longer than across the river. The same 3:1 directional anisotropy was also seen in Cd and Zn.

Figure 6 shows the distance from-the-river trend for Pb. Higher concentrations of the element are observed closer to the river, with a decreasing trend moving outward. The modeled trend indicates a gradual stabilization of concentrations beyond 10,000 m from the river.

Figure 7 shows the trend along-the-river exhibiting a gradual decay in concentrations, but there is also evidence of fluctuations, indicated by spikes in local locations such as Northport and Bossburg. The trends for Cd and Zn demonstrate similar overall patterns.

Locally Varying Anisotropy

Figure 8 demonstrates a flexible grid system designed to capture locally varying anisotropy along and away from the Upper Columbia River. The reliability of estimates will be improved by a grid design that captures the geometry of the local trends and environmental characteristics influenced by directional processes.

The flexible grid was generated based on two primary directional influences; distance from the river, where the zero location is the centreline of the river, and distance along the river, where the zero location is where the river crosses the Canada-US border.

When the Easting (X) and Northing (Y) are used directly for the local trend calculations that UK will do, the resulting maps are not as coherent as they are when Distance-from-the-river (X') and Distance-along-the-river (Y') are used instead. This amounts to locally rotating the XY coordinate system so that X'Y' always line up with the river.

UK could also incorporate concentration trends in elevation where there appears to be a decrease in metal concentrations in samples

[2] Subset II has a range of 250 m with a high nugget effect of 0.9; the range of Subset I is three times longer at 750 m and a lower nugget effect of 0.6.

taken higher up the slopes of the ridges that form the Columbia River valley. This possibility was tested for these studies but not implemented for the final maps because the use of the locally rotated X'Y' coordinates has the beneficial effect of elevation changes being picked up in the distance from-the-river coordinate (X').

Box-Cox Transformation

The Box-Cox transformation is a statistical technique (Box and Cox, 1964) used to make data more closely approximate a normal distribution. SGS applies to data that follow a normal distribution (the classical "bell-shaped" curve). Applying the Box-Cox transformation to the Pb-Cd-Zn data sets enables SGS to produce more reliable estimates.

The Box-Cox transformation is defined as:

$$T(p) = \frac{C^p - 1}{p} \text{ for } p \neq 0$$
$$T(p) = \ln(C) \text{ for } p = 0$$

where *C* represents the observed concentration values, *p* is an adjustable parameter that depends on the skewness of the original data, and *T* is the transformed Box-Cox value.

For this study, the Box-Cox transformation was applied locally to Pb, Cd, and Zn to reduce skewness and achieve a more normal-like (or "Gaussian") distribution with the optimal *p* value determined globally for each element. The use of a local transformation based on the closest 30 samples allows the SGS simulations to locally customize the uncertainty distributions to local data. This avoids unduly smearing high values into areas with low concentrations and vice versa.

The optimal *p* for Cd and Zn was 0, meaning a log transformation was most suitable. The optimal *p* for Pb was -0.1, indicating that a mild inverse transformation was required to achieve normality. The transformation significantly reduced the skewness, normalizing the data set and improving statistical assumptions for further analysis.

Variograms

To determine the spatial continuity of variograms in the trend directions, experimental variograms were calculated in the along-river and across-river distance directions, using the Box-Cox transformed residual values. When the Easting (X) and Northing (Y) values were used for this, the graphs weren't as coherent as the graphs produced using the more flexible distance-from-the-river (X') and distance-along-the-river (Y').

Table 4 shows the variogram model parameters used in the estimation. Of these user-selected parameters, the two with the greatest influence on the maps are: the relative nugget effect and the directional anisotropy, which is the ratio of the along-the-river range to the from-the-river range.

The relative nugget effect quantifies variability at very short scales. It is a combination of imprecision due to the variability of laboratory measurements and due to genuine in-situ short-scale variations in soil concentrations. For areas within the OU 3 study area, where aerial deposition is understood to be the primary source of regional scale elevated Pb, Cd, and Zn concentrations in surface soil, the in-situ short-scale variability should be smaller than the variability of laboratory measurements. Field duplicate samples were extracted from the Subset I data set for all Pb, Cd, and Zn samples, and using the Box-Cox transform, the variance of differences between duplicate pairs was used as the minimum relative nugget effect for each element. The relative nugget effects are high for all three metals, close to 50%. This is because the variance of laboratory duplicates is also high for all three metals. These high short-scale variabilities have two consequences:

- The predicted concentrations exhibit a high degree of uncertainty due to the variability exhibited in the data set. With

half of the fluctuations seen over the entire data set being seen in duplicate pairs taken at essentially the same location, any estimate, no matter what methodology is used, is going to have poor precision due to the imprecision in the data themselves.

- The benefit of additional sampling in high-uncertainty areas is limited by the fact that new laboratory measurements are expected to have the same imprecision as historical measurements. The key to reducing uncertainty is to do multiple lab measurements of the same sample material so that imprecision is reduced through the averaging of duplicate measurements. The collection of additional individual samples is unlikely to significantly reduce large-scale uncertainty within the UCR study area.

The importance of local directional anisotropy is that local estimates will assign more weight to nearby samples that are parallel to the river and less weight to those that are perpendicular to the river. Contour lines of the mapped concentrations will tend to run parallel to the river, following it around bends.

Post-Processing

Outputted Maps

Following the validation of the simulated models, post-processing steps are performed to generate statistical summaries and visual representations of simulation outcomes. This report includes three primary output maps:

- The median of simulated values at any location serves as the prediction for unknown Pb-Cd-Zn concentrations at that location (Maps 4, 5, and 6).
- Uncertainty is summarized using the spread between the 10th and 90th percentiles of 100 simulated values (Maps 7, 8, and 9).
- Probabilities of exceeding defined thresholds are calculated by counting, at each location, the number of times (out of 100 simulations) the simulated value exceeds the threshold (Maps 10 - 15).

Cross Validation

For the Subset I samples in the United States, cross-validation was conducted using the "one-at-a-time" method to assess the effectiveness of the interpolation procedure. This involved sequentially removing one sample, re-estimating its element concentration using the remaining samples, and comparing the predicted value to the actual measurement.

Tables 5 - 7 show a comparison of the summary statistics of each element. In each metal, the statistics show good agreement between the measured and the predicted values.

Visual Validation Checks

Several visual validation checks were performed. One involved visually inspecting simulated concentration maps against actual sample measurements. Specifically, simulated concentrations were compared to field-measured values to confirm consistency in patterns and spatial distributions.

Another check of the maps is shown in Figure 9, which shows the Pb, Cd, and Zn maps side-by-side. Even though the three elements were not estimated as a cross-correlated set and no regional trends were used, the mapping methodology, especially the use of UK with distance along-the-river and across-the-river coordinates, produces a set of three maps that show broad similarities: concentrations tend to be higher at the US-Canada border and to decrease to the southwest, following the river valley.

Statistical Validation Checks

Although cross-validation studies are usually summarized by correlation coefficients and global averages, for a mapping task that may

eventually inform RI decision-making, an analysis of misclassification provides additional relevant information.

Tables 8 - 16 show the misclassification rates among the elements and the provided thresholds. Figures 10, 11, and 12 show scatter plots for cross-validation of the three metals. These tables and figures show a high correlation between predicted and actual values and low misclassification errors at the chosen thresholds.

Conclusion

Probabilistic models mapping Pb, Cd, and Zn concentrations were developed using Universal Kriging and Sequential Gaussian Simulation, which are robust geostatistical techniques that have been used in environmental studies for decades. Following model development, validation procedures compared simulation outputs to original input data to verify accuracy. These included cross-validation as well as visual and statistical checks. Cross-validation confirmed good agreement between measured and predicted values, visual checks showed consistency between the patterns and spatial distributions for all three metals, and low misclassification errors for the statistical checks at each chosen threshold.

These validation metrics collectively demonstrated the models' ability to predict surface metal distributions. To facilitate interpretation, post-processing workflows generated:

- Statistical summaries quantifying metal concentration ranges
- Spatial probability maps highlighting areas with elevated concentrations in surface soil
- Maps visualizing predicted uncertainties

Maps

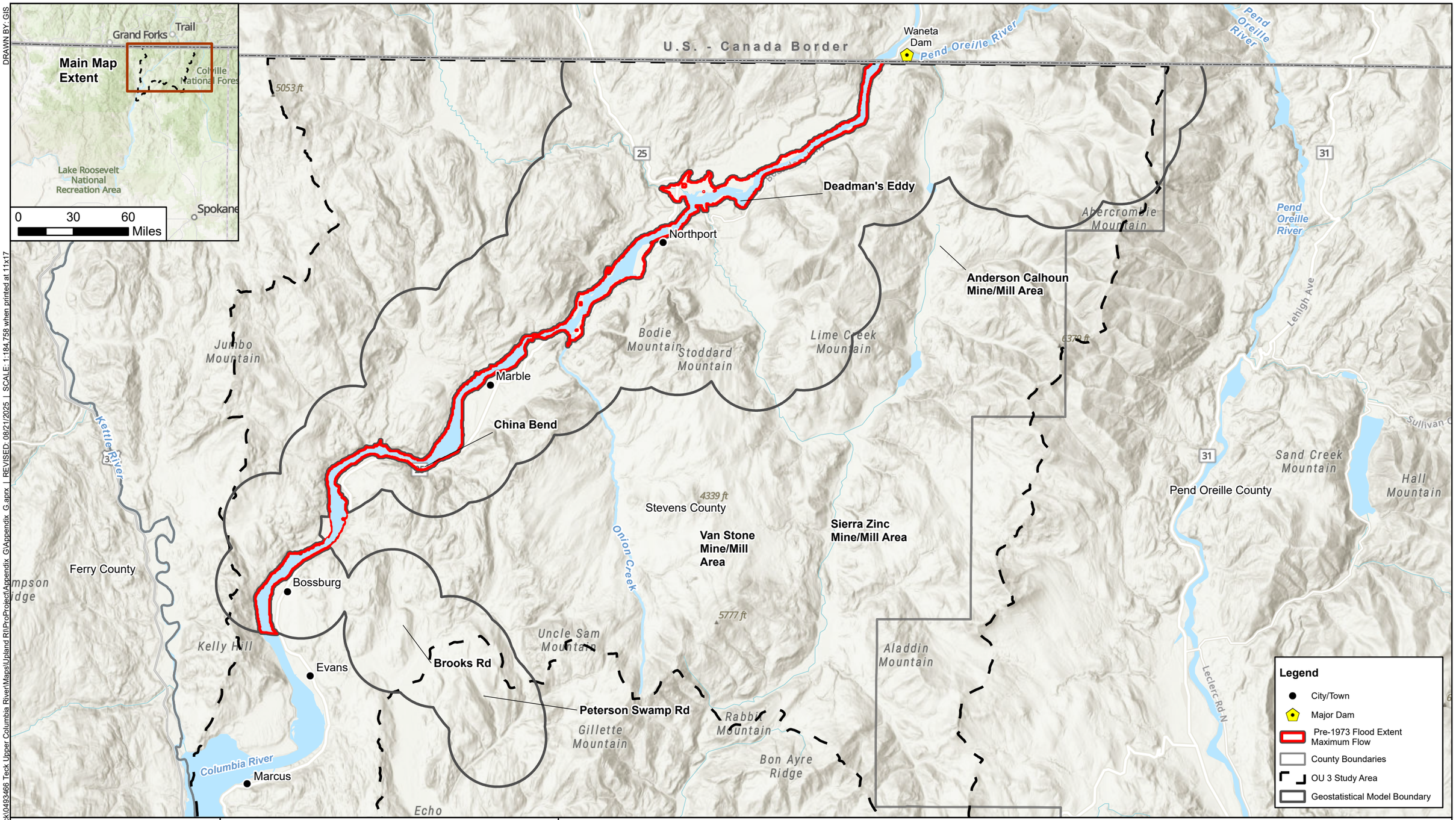

ERM
Environmental Resources Management
www.erm.com

0 1.5 3 6 Miles

N

Map 1. **Geostatistical Model Boundary**
Final Upland RI Report
Upper Columbia River, Washington

Source: Esri - World Topographic Map; NAD 1983 UTM Zone 11N

DRAWN BY: GIS | REVISED: 08/21/2025 | SCALE: 1:184,758 when printed at 11x17

FILE: M:\US\Projects\S-U\Teck\0493466 Teck Upper Columbia River\Maps\Upland RI\ProProject\Appendix G\Appendix G.aprx

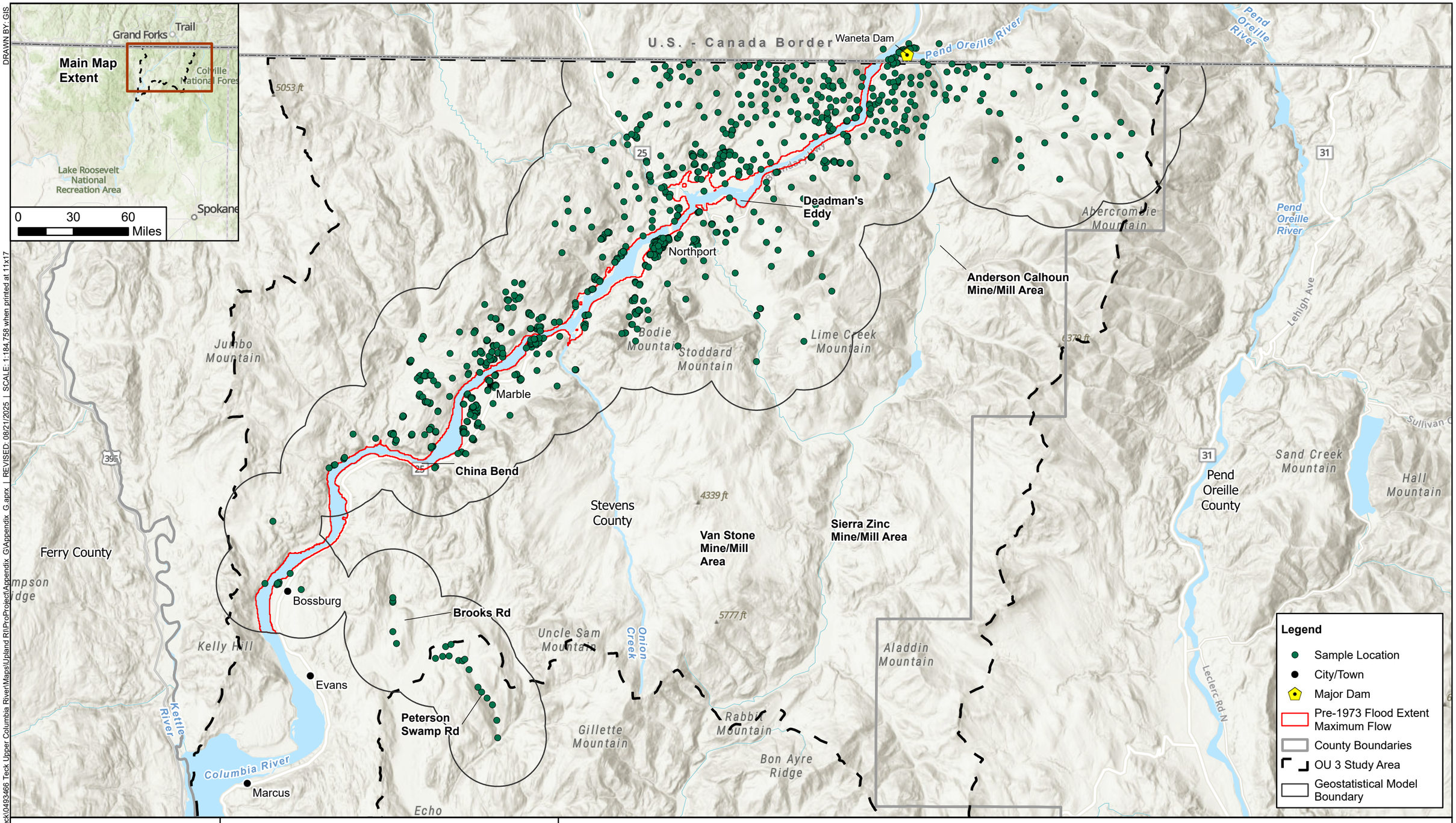

ERM
Environmental Resources Management
www.erm.com

0 1.5 3 6 Miles

N

Map 2. **Surface Soil Sample Locations Used in the Geostatistical Model (Subset I)**
Final Upland RI Report
Upper Columbia River, Washington

Source: Esri - World Topographic Map; NAD 1983 UTM Zone 11N

DRAWN BY: GIS | REVISED: 08/21/2025 | SCALE: 1:184,758 when printed at 11x17

FILE: M:\US\Projects\S-U\Teck\0493466 Teck Upper Columbia River\Maps\Upland RI\ProProject\Appendix G\Appendix G.aprx

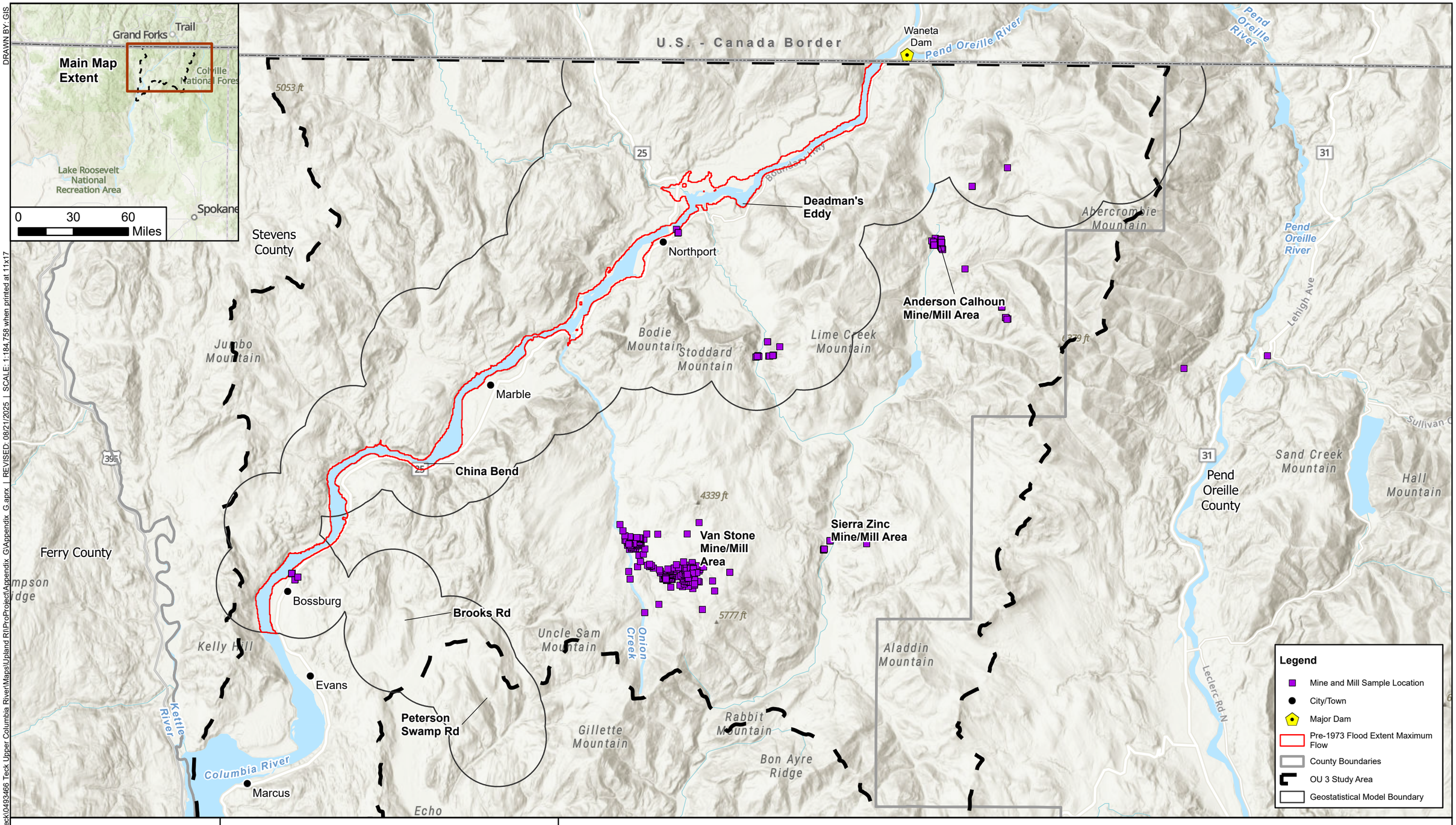

ERM
Environmental Resources Management
www.erm.com

Map 3. **Mines and Mills Sample Locations (Subset II)**
Final Upland RI Report
Upper Columbia River, Washington

Source: Esri - World Topographic Map; NAD 1983 UTM Zone 11N

DRAWN BY: GIS
FILE: M:\US\Projects\S-U\Teck\0493466 Teck Upper Columbia River\Maps\Upland RI\ProProject\Appendix GA\Appendix G.aprx | REVISED: 08/21/2025 | SCALE: 1:184,758 when printed at 11x17

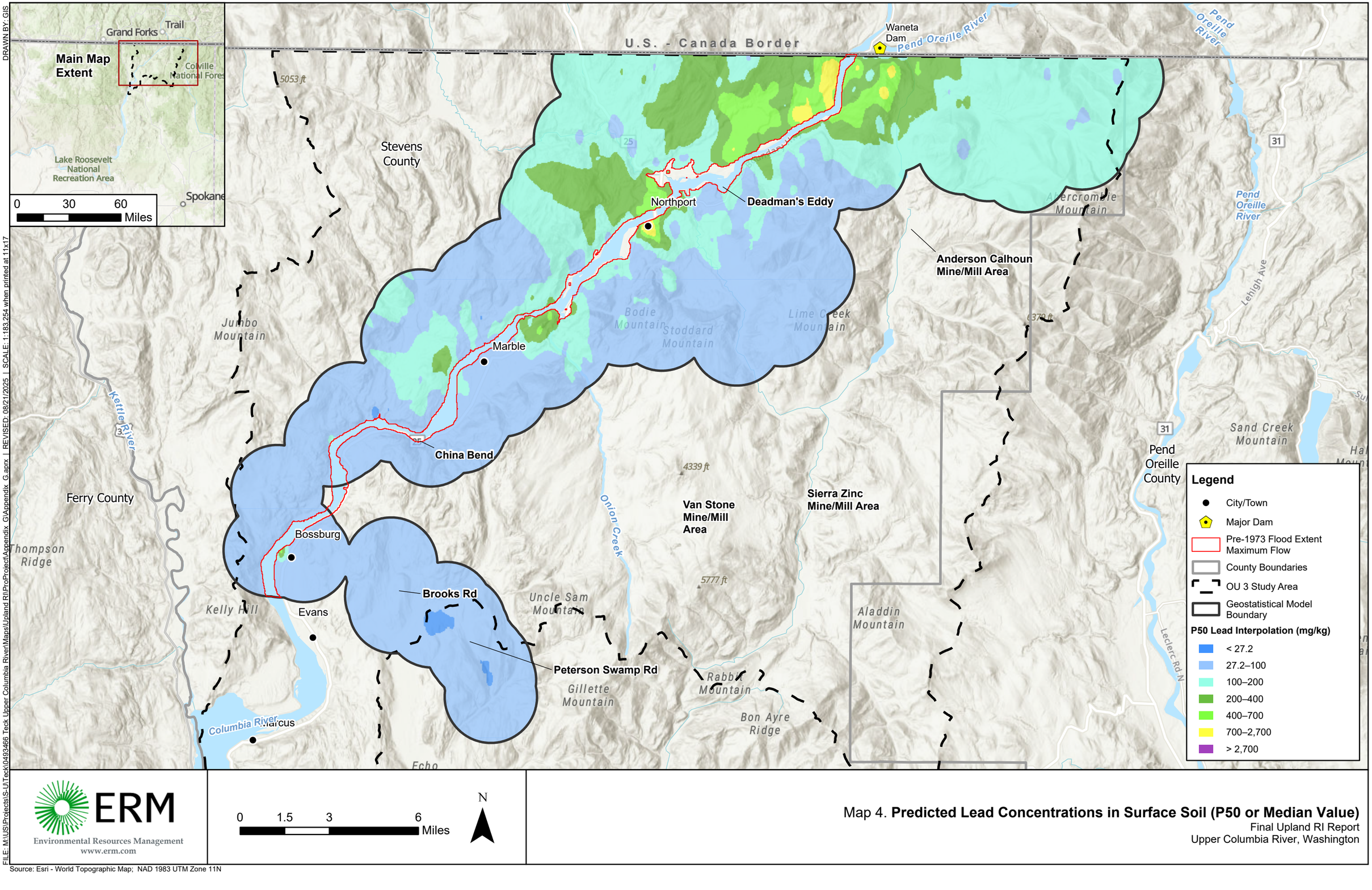

ERM
Environmental Resources Management
www.erm.com

Map 4. **Predicted Lead Concentrations in Surface Soil (P50 or Median Value)**
Final Upland RI Report
Upper Columbia River, Washington

Source: Esri - World Topographic Map; NAD 1983 UTM Zone 11N

DRAWN BY: GIS | REVISED: 08/21/2025 | SCALE: 1:183,254 when printed at 11x17
FILE: M:\US\Projects\S-U\Teck\0493466 Teck Upper Columbia River\Maps\Upland RI\ProProject\Appendix GV\Appendix G.aprx

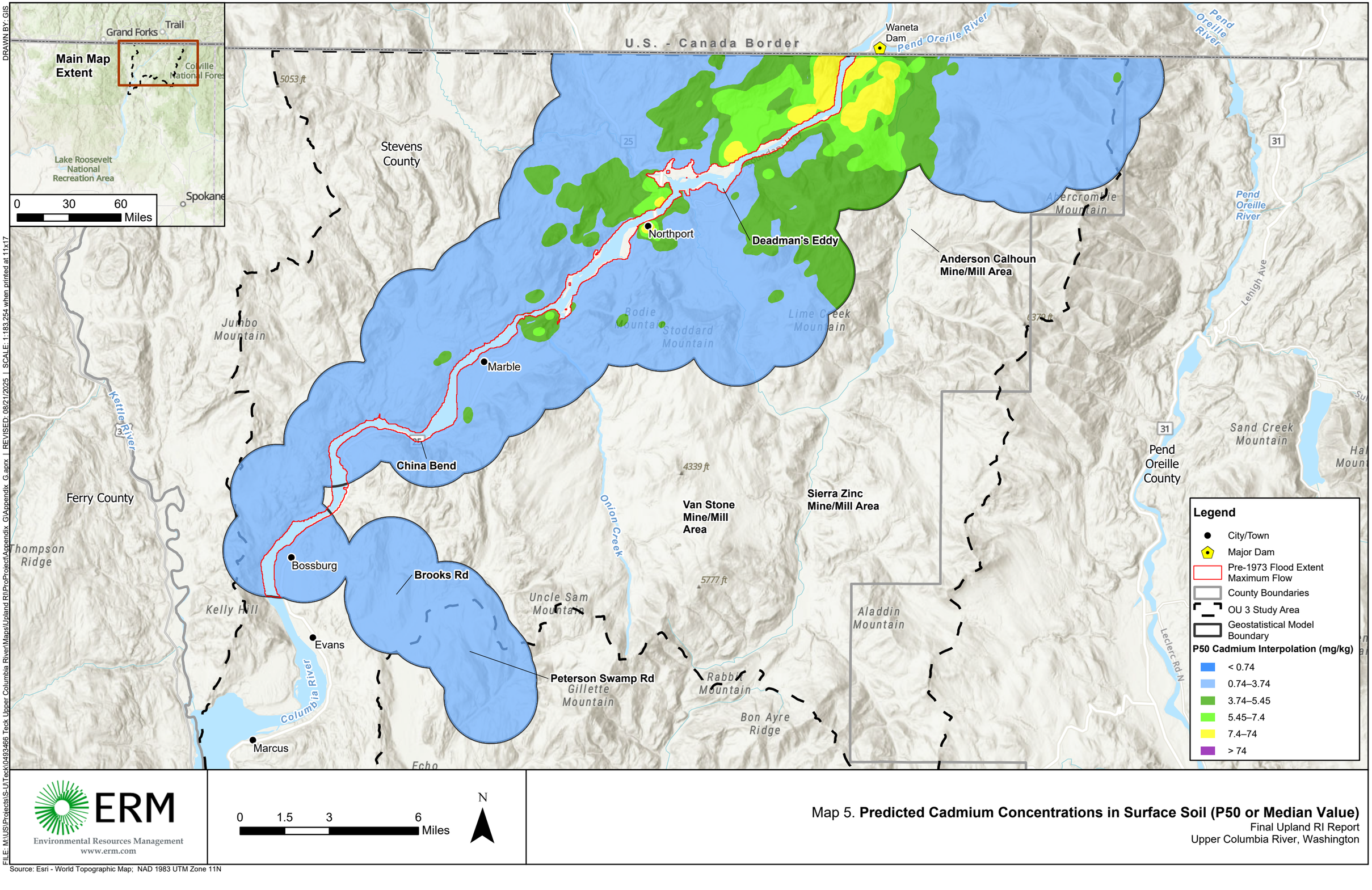

ERM
Environmental Resources Management
www.erm.com

Map 5. **Predicted Cadmium Concentrations in Surface Soil (P50 or Median Value)**
Final Upland RI Report
Upper Columbia River, Washington

Source: Esri - World Topographic Map; NAD 1983 UTM Zone 11N

DRAWN BY: GIS
FILE: M:\US\Projects\S-U\Teck\0493466 Teck Upper Columbia River\Maps\Upland RI\ProProject\Appendix GV\Appendix G.aprx | REVISED: 08/21/2025 | SCALE: 1:183,254 when printed at 11x17

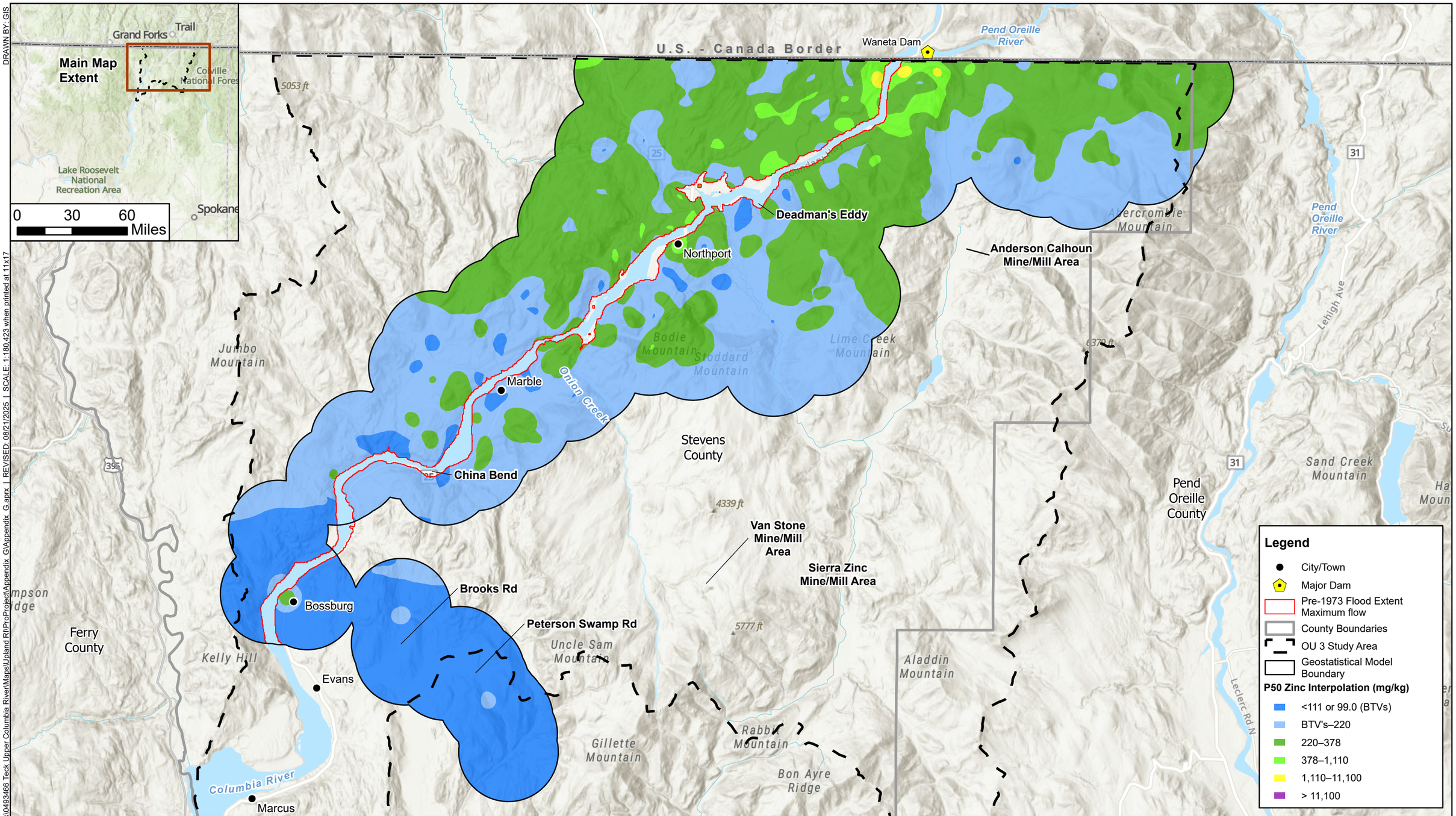

ERM
Environmental Resources Management
www.erm.com

0 1.25 2.5 5 Miles

N

Map 6. **Predicted Zinc Concentrations in Surface Soil (P50 or Median Value)**
Final Upland RI Report
Upper Columbia River, Washington

Source: Esri - World Topographic Map; NAD 1983 UTM Zone 11N

DRAWN BY: GIS | REVISED: 08/21/2025 | SCALE: 1:180,423 when printed at 11x17

FILE: M:\US\Projects\S-U\Teck\0493466 Teck Upper Columbia River\Maps\Upland RI\ProProject\Appendix GVAppendix G.aprx

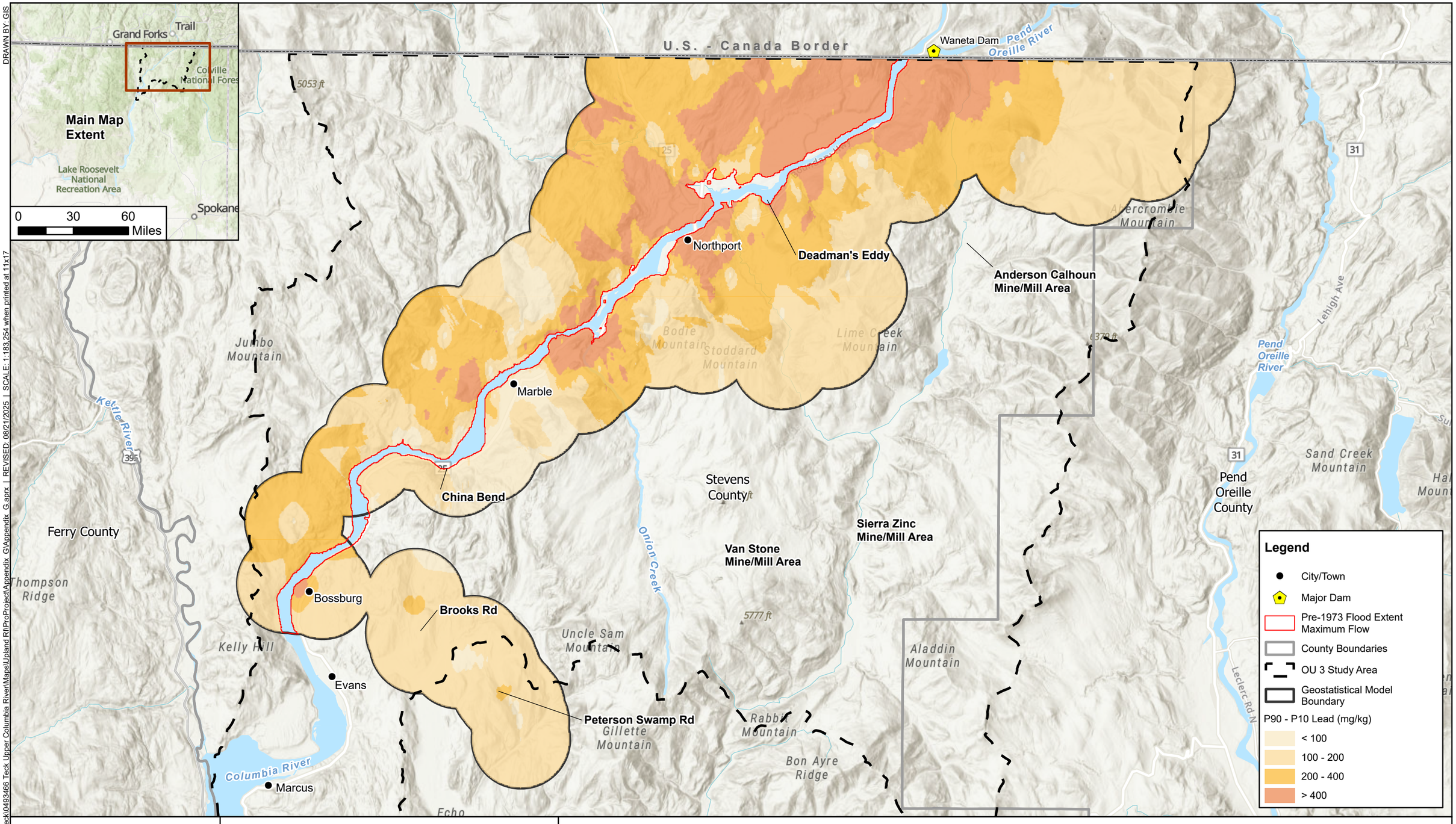

ERM
Environmental Resources Management
www.erm.com

0 1.25 2.5 5 Miles

N

Map 7. **Uncertainty in Predicted Lead Concentrations in Surface Soil (P90 Minus P10)**
Final Upland RI Report
Upper Columbia River, Washington

Source: Esri - World Topographic Map; NAD 1983 UTM Zone 11N

DRAWN BY: GIS | REVISED: 08/21/2025 | SCALE: 1:183,254 when printed at 11x17 | FILE: M:\US\Projects\S-U\Teck\0493466 Teck Upper Columbia River\Maps\Upland RI\ProProject\Appendix GV\Appendix G.aprx

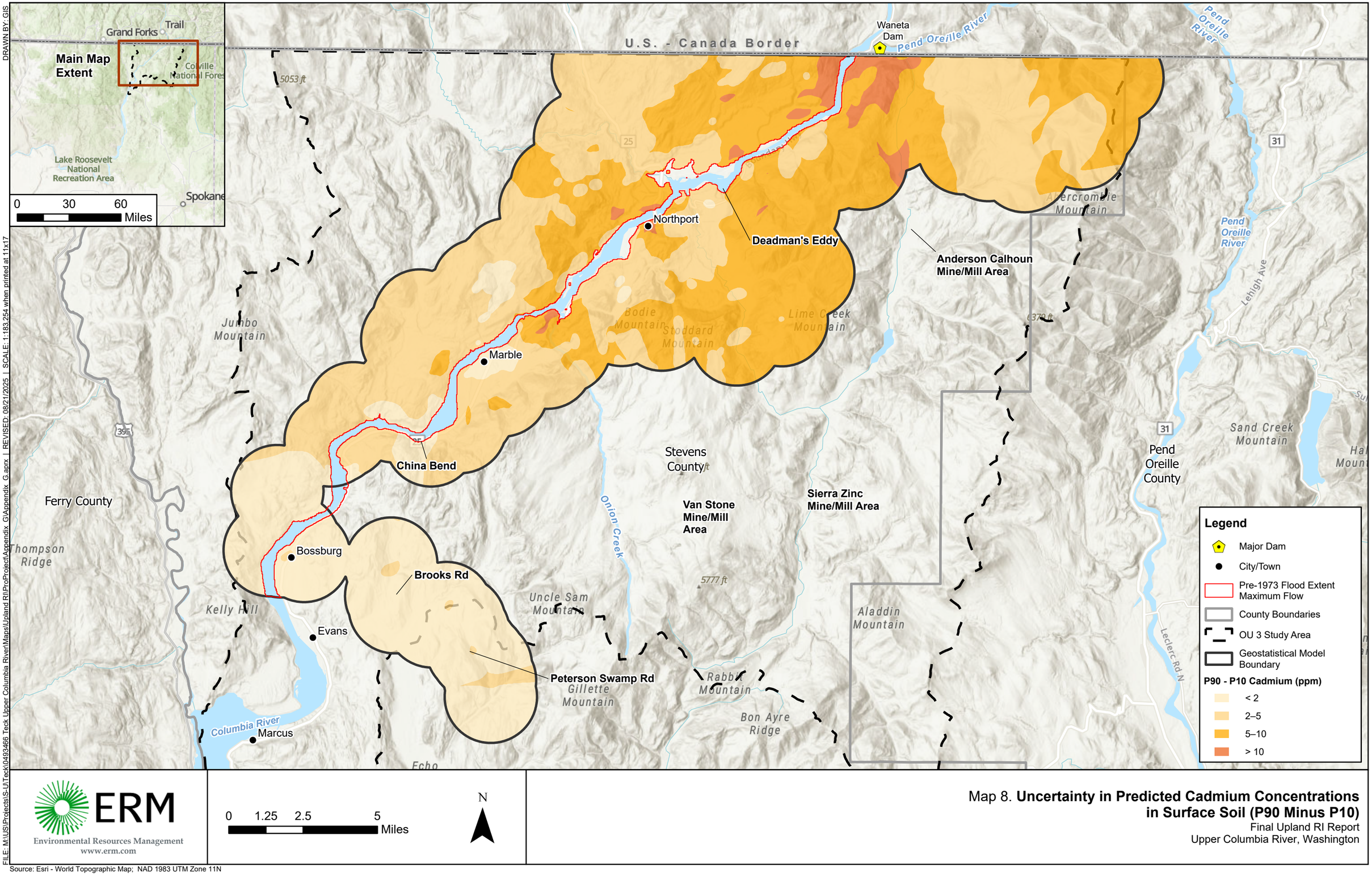

ERM
Environmental Resources Management
www.erm.com

Map 8. **Uncertainty in Predicted Cadmium Concentrations in Surface Soil (P90 Minus P10)**
Final Upland RI Report
Upper Columbia River, Washington

Source: Esri - World Topographic Map; NAD 1983 UTM Zone 11N

DRAWN BY: GIS
FILE: M:\US\Projects\S-U\Teck\0493466 Teck Upper Columbia River\Maps\Upland RI\ProProject\Appendix GV\Appendix G.aprx | REVISED: 08/21/2025 | SCALE: 1:183,254 when printed at 11x17

DRAWN BY: GIS

FILE: M:\US\Projects\S-U\Teck\0493466 Teck Upper Columbia River\Maps\Upland RI\ProProject\Appendix G\Appendix G.aprx | REVISED: 08/21/2025 | SCALE: 1:183,254 when printed at 11x17

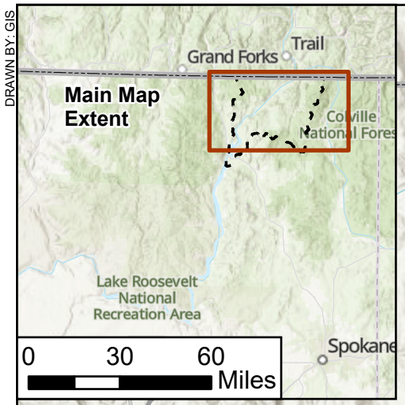

U.S. - Canada Border

Waneta Dam

Pend Oreille River

Northport

Deadman's Eddy

Marble

Onion Creek

Columbia River

China Bend

Bossburg

Brooks Rd

Peterson Swamp Rd

Evans

Marcus

Anderson Calhoun Mine/Mill Area

Van Stone Mine/Mill Area

Sierra Zinc Mine/Mill Area

Stevens County

Pend Oreille County

Ferry County

Jumbo Mountain

Bodie Mountain

Stoddard Mountain

Lime Creek Mountain

Abercrombie Mountain

Sand Creek Mountain

Thompson Ridge

Kelly Hill

Uncle Sam Mountain

Gillette Mountain

Rabbit Mountain

Bon Ayre Ridge

Aladdin Mountain

Lehigh Ave

Leclerc Rd N

5053 ft

4339 ft

5777 ft

6239 ft

25

31

395

Echo

Legend

- City/Town
- Major Dam
- Pre-1973 Flood Extent Maximum flow
- County Boundaries
- OU 3 Study Area
- Geostatistical Model Boundary

P90 - P10 Zn (ppm)

- < 100
- 100–200
- 200–400
- > 400

ERM
Environmental Resources Management
www.erm.com

0 1.25 2.5 5
Miles

N

Map 9. **Uncertainty in Predicted Zinc Concentrations in Surface Soil (P90 Minus P10)**
Final Upland RI Report
Upper Columbia River, Washington

Source: Esri - World Topographic Map; NAD 1983 UTM Zone 11N

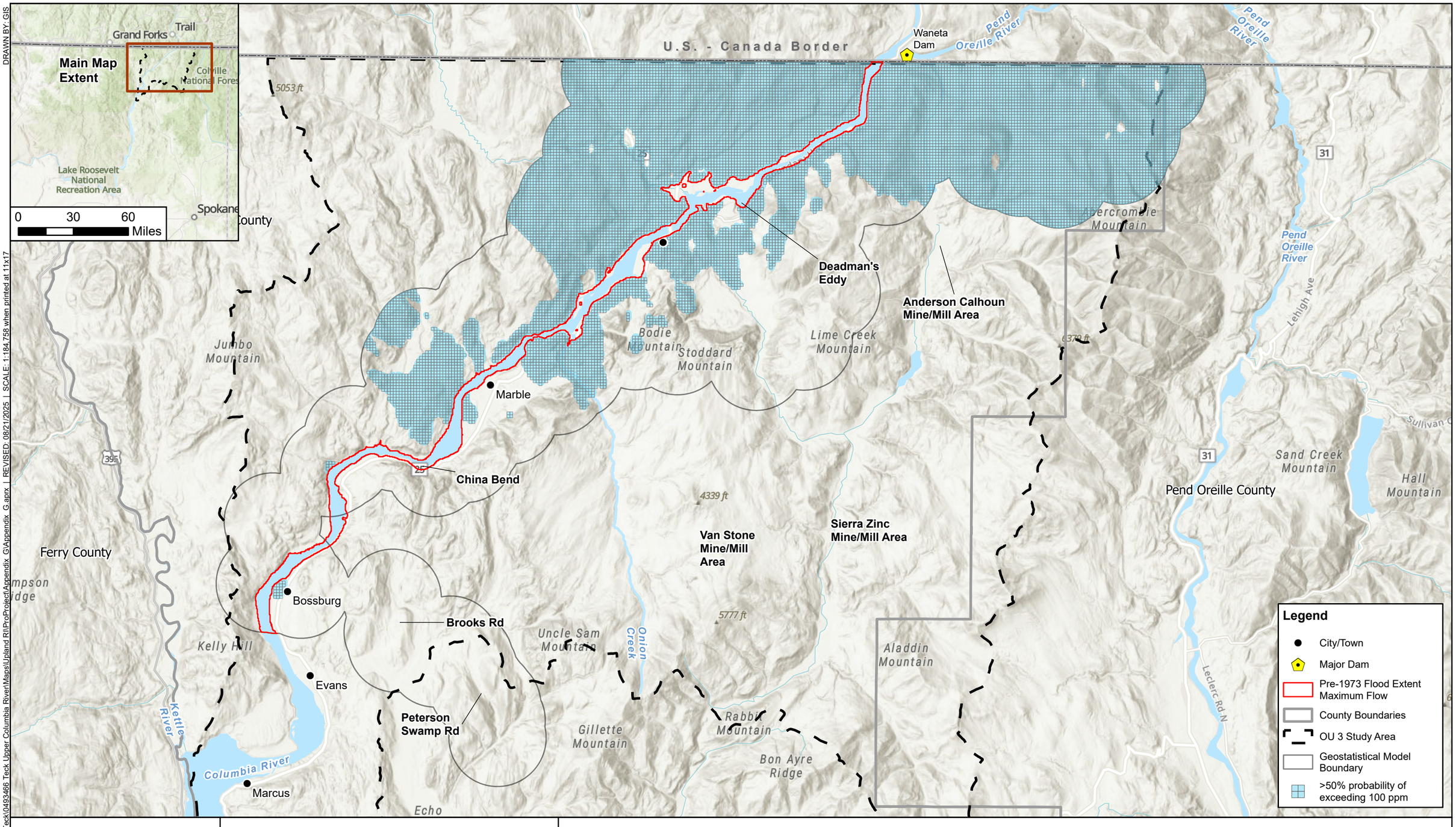

DRAWN BY: GIS

FILE: M:\US\Projects\S-U\Teck\0493466 Teck Upper Columbia River\Maps\Upland RI\ProProject\Appendix GVAppendix G.aprx | REVISED: 08/21/2025 | SCALE: 1:184,758 when printed at 11x17

ERM
Environmental Resources Management
www.erm.com

0 1.5 3 6 Miles

N

Map 10. **Area with >50% Probability of Exceeding 100 ppm Lead in Surface Soil**
Final Upland RI Report
Upper Columbia River, Washington

Source: Esri - World Topographic Map; NAD 1983 UTM Zone 11N

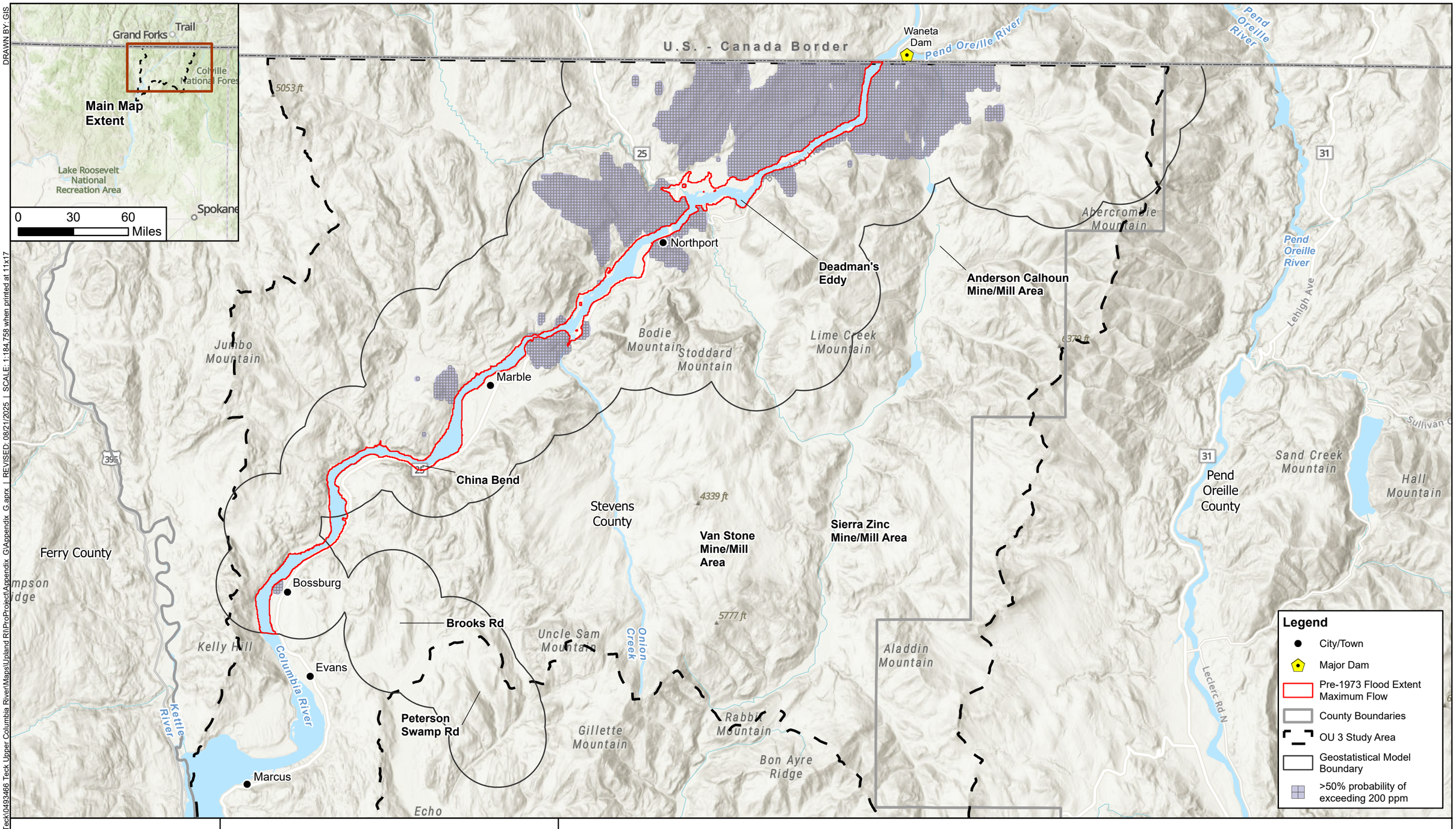

ERM
Environmental Resources Management
www.erm.com

0 1.5 3 6 Miles

N

Map 11. **Area with >50% Probability of Exceeding 200 ppm Lead in Surface Soil**
Final Upland RI Report
Upper Columbia River, Washington

Source: Esri - World Topographic Map; NAD 1983 UTM Zone 11N

DRAWN BY: GIS | REVISED: 08/21/2025 | SCALE: 1:184,758 when printed at 11x17 | FILE: M:\US\Projects\S-U\Tex\0493466 Teck Upper Columbia River\Maps\Upland RI\ProProject\Appendix GA\Appendix G.aprx

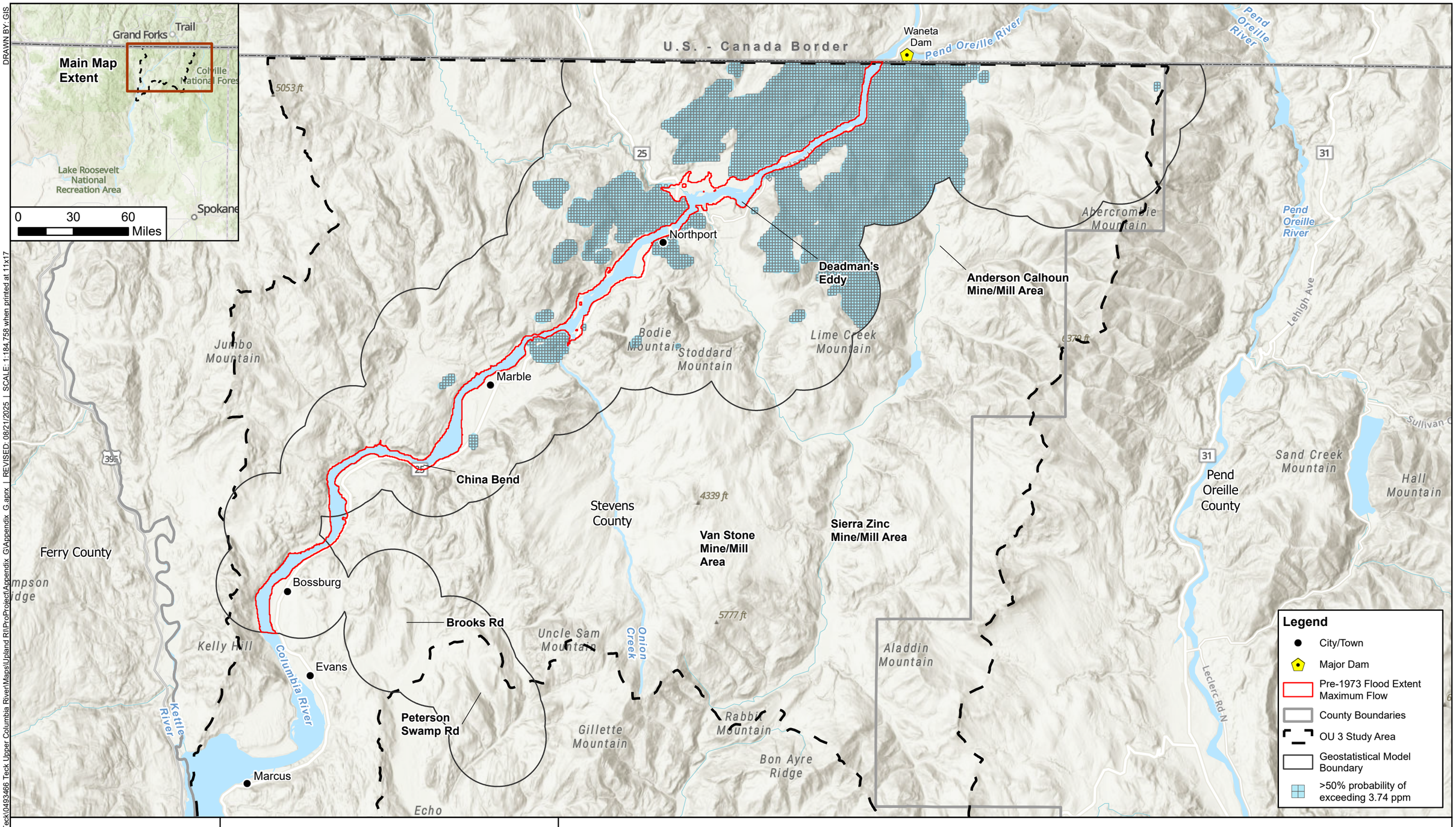

ERM
Environmental Resources Management
www.erm.com

0 1.5 3 6 Miles

N

Map 12. **Area with >50% Probability of Exceeding 3.74 ppm Cadmium in Surface Soil**
Final Upland RI Report
Upper Columbia River, Washington

Source: Esri - World Topographic Map; NAD 1983 UTM Zone 11N

DRAWN BY: GIS | REVISED: 08/21/2025 | SCALE: 1:184,758 when printed at 11x17 | FILE: M:\US\Projects\S-U\Teck\0493466 Teck Upper Columbia River\Maps\Upland RI\ProProject\Appendix GA\Appendix G.aprx

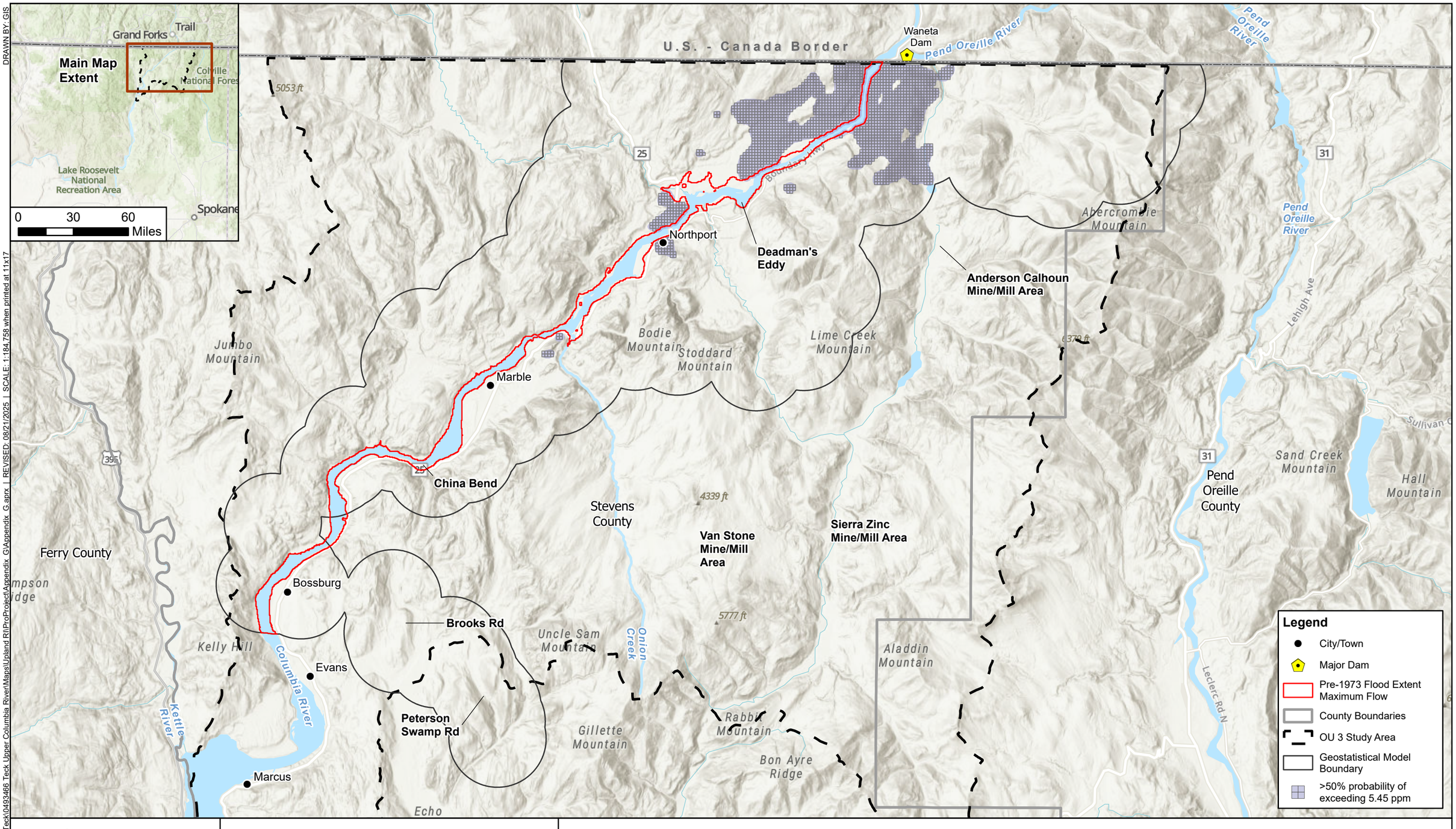

ERM
Environmental Resources Management
www.erm.com

Map 13. **Area with >50% Probability of Exceeding 5.45 ppm Cadmium in Surface Soil**
Final Upland RI Report
Upper Columbia River, Washington

Source: Esri - World Topographic Map; NAD 1983 UTM Zone 11N

DRAWN BY: GIS
FILE: M:\US\Projects\S-U\Tex\0493466 Teck Upper Columbia River\Maps\Upland RI\ProProject\Appendix GV\Appendix G.aprx | REVISED: 08/21/2025 | SCALE: 1:184,758 when printed at 11x17

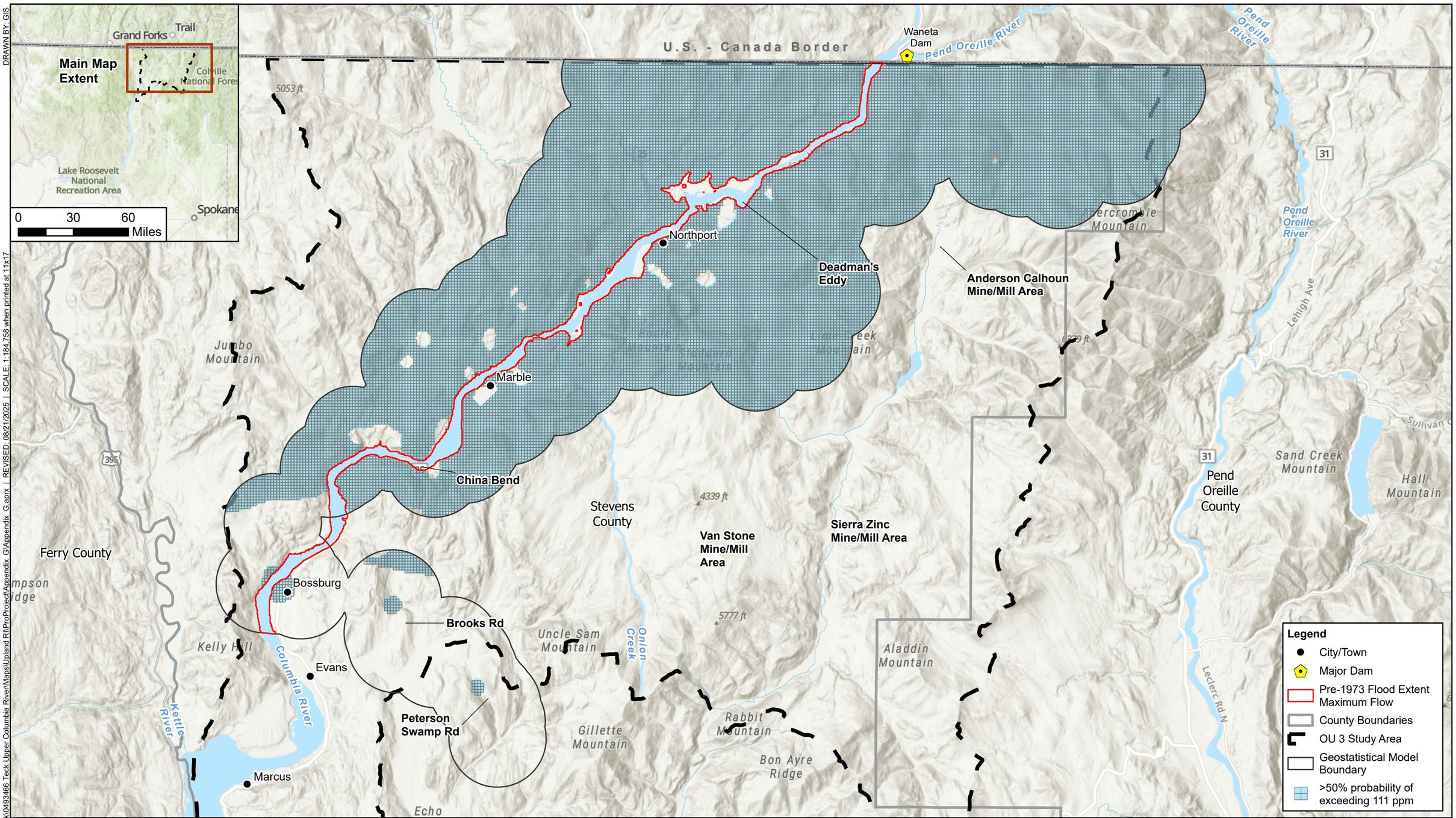

ERM
Environmental Resources Management
www.erm.com

Map 14. **Area with >50% Probability of Exceeding 111 ppm Zinc in Surface Soil**
Final Upland RI Report
Upper Columbia River, Washington

Source: Esri - World Topographic Map; NAD 1983 UTM Zone 11N

DRAWN BY: GIS
FILE: M:\US\Projects\S-U\Teck\0493466 Teck Upper Columbia River\Maps\Upland RI\ProProject\Appendix GVAppendix G.aprx | REVISED: 08/21/2025 | SCALE: 1:184,758 when printed at 11x17

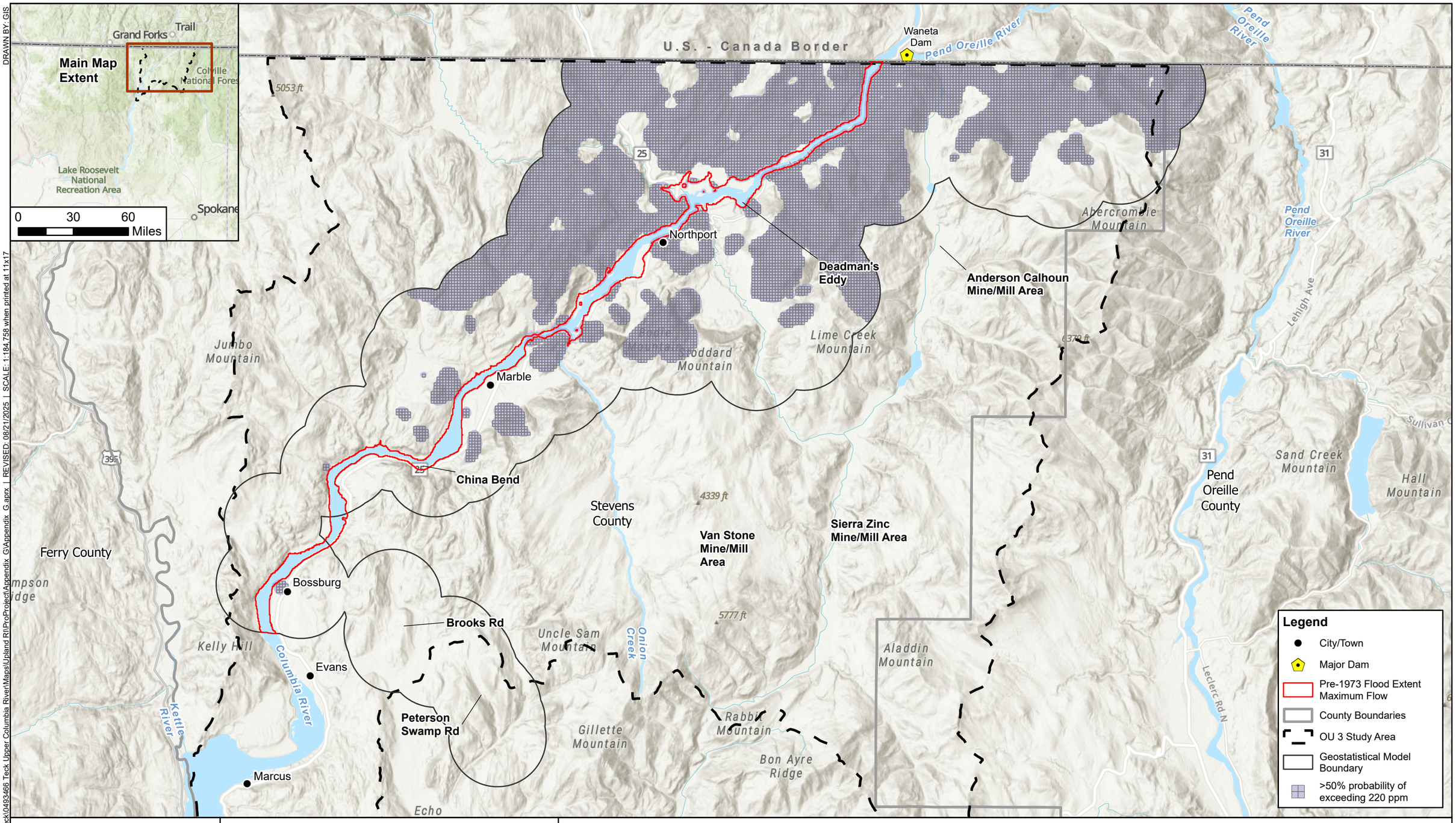

ERM
Environmental Resources Management
www.erm.com

0 1.5 3 6 Miles

N

Map 15. **Area with >50% Probability of Exceeding 220 ppm Zinc in Surface Soil**
Final Upland RI Report
Upper Columbia River, Washington

Source: Esri - World Topographic Map; NAD 1983 UTM Zone 11N

DRAWN BY: GIS | REVISED: 08/21/2025 | SCALE: 1:184,758 when printed at 11x17

FILE: M:\US\Projects\S-U\Teck\0493466 Teck Upper Columbia River\Maps\Upland RI\ProProject\Appendix G\Appendix G.aprx

Figures

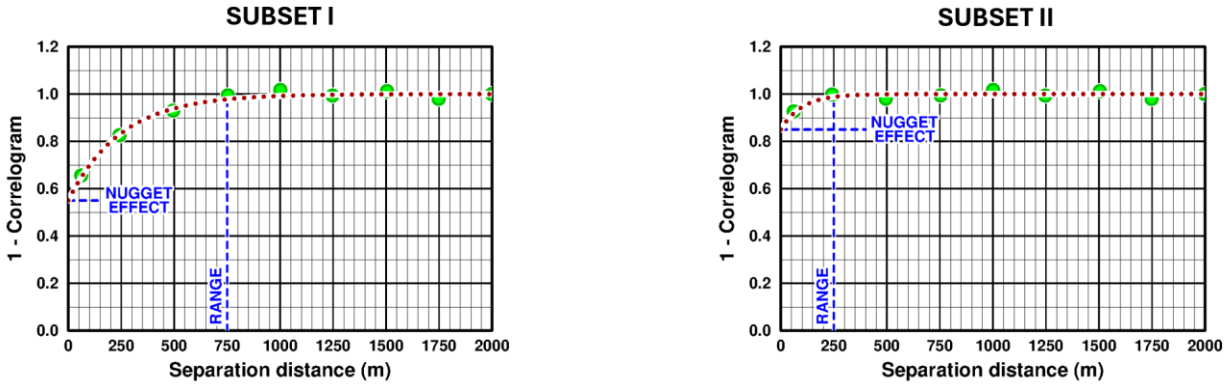

Figure 1 - Variograms showing differences in nugget effect and range between the Subsets of Pb

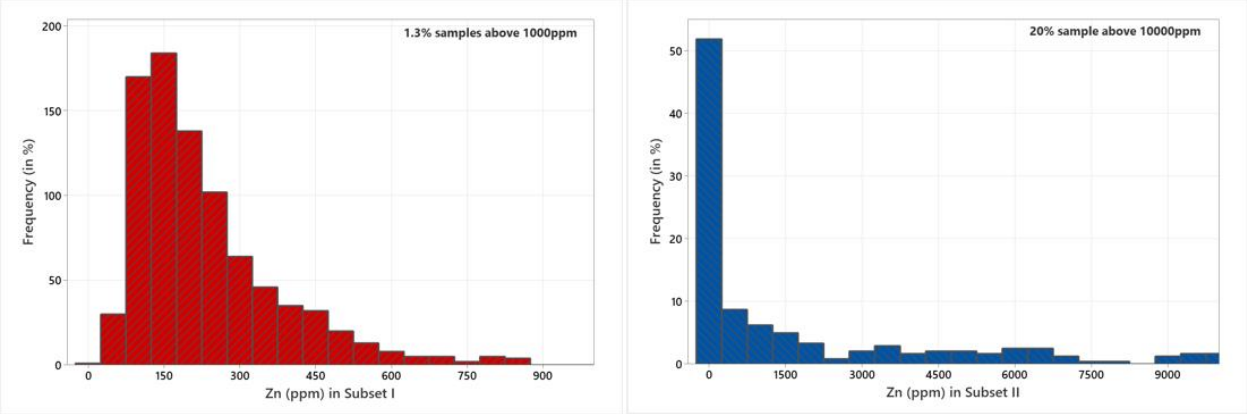

Figure 2 - Histogram showing the distribution of Pb samples in Subsets I and II

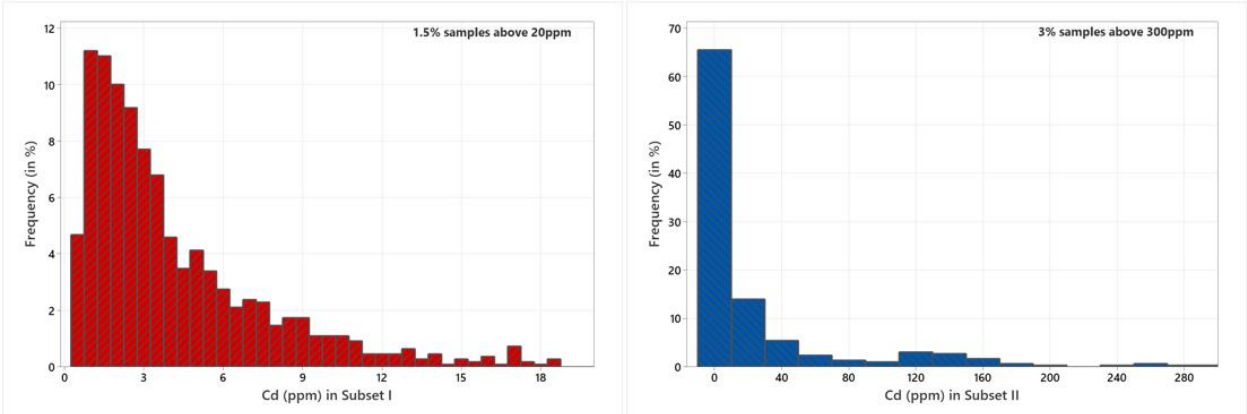

Figure 3 - Histogram showing the distribution of Cd samples in Subsets I and II

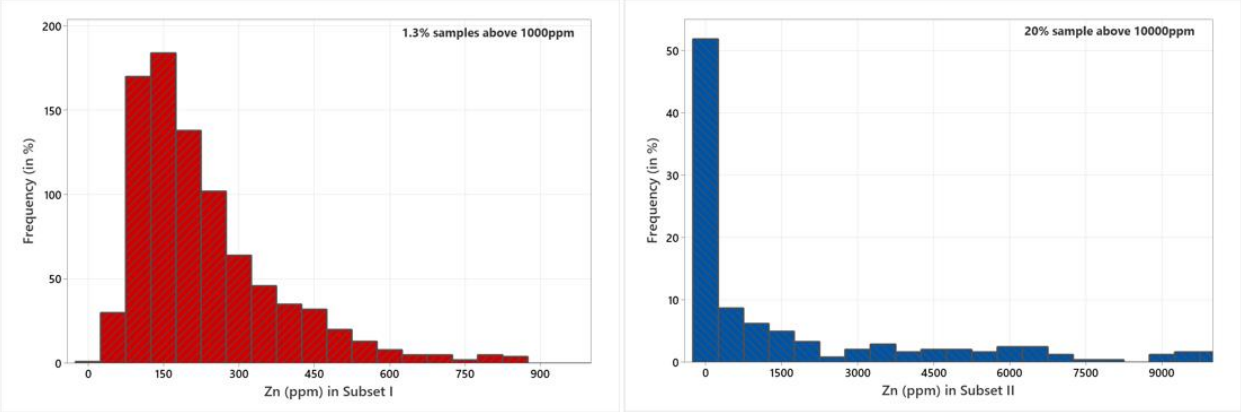

Figure 4 - Histogram showing the distribution of Zn samples in Subsets I and II

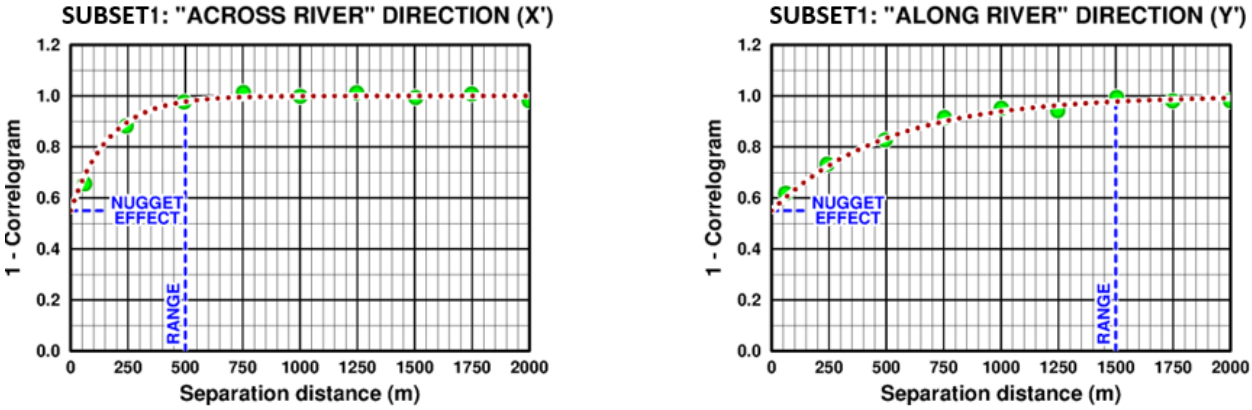

Figure 5 - Variograms showing the ranges differences relative to river

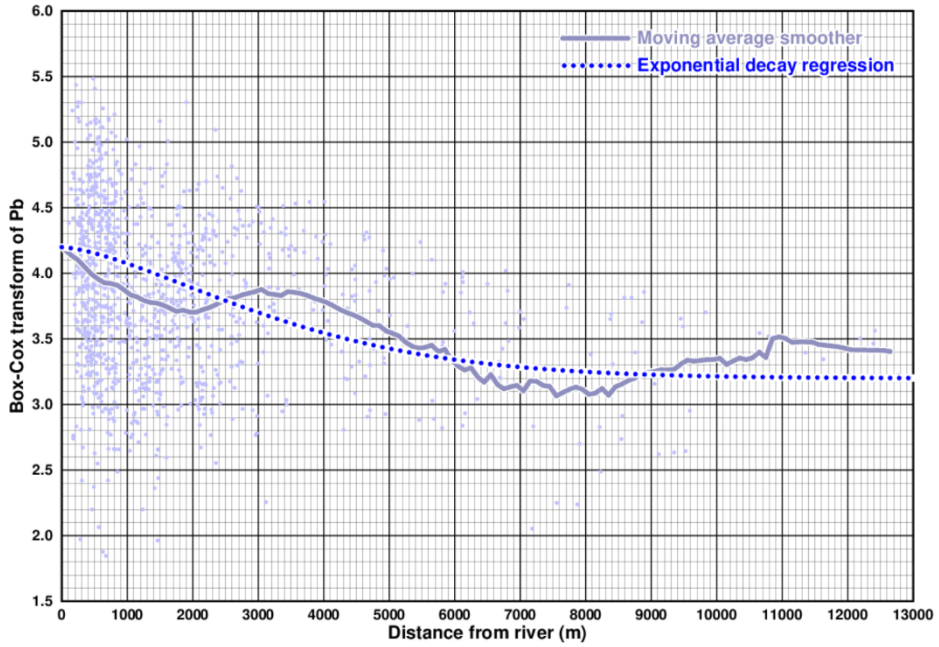

Figure 6 - Trend in Box-Cox transform of Pb with distance-from-river

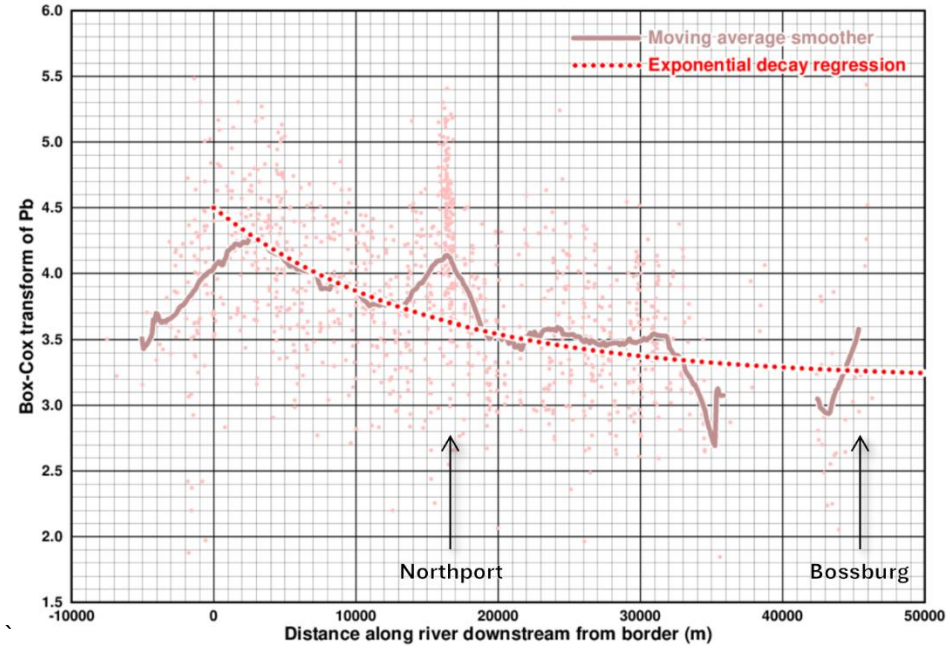

Figure 7 - Trend in Box-Cox transform of Pb with distance-along-river

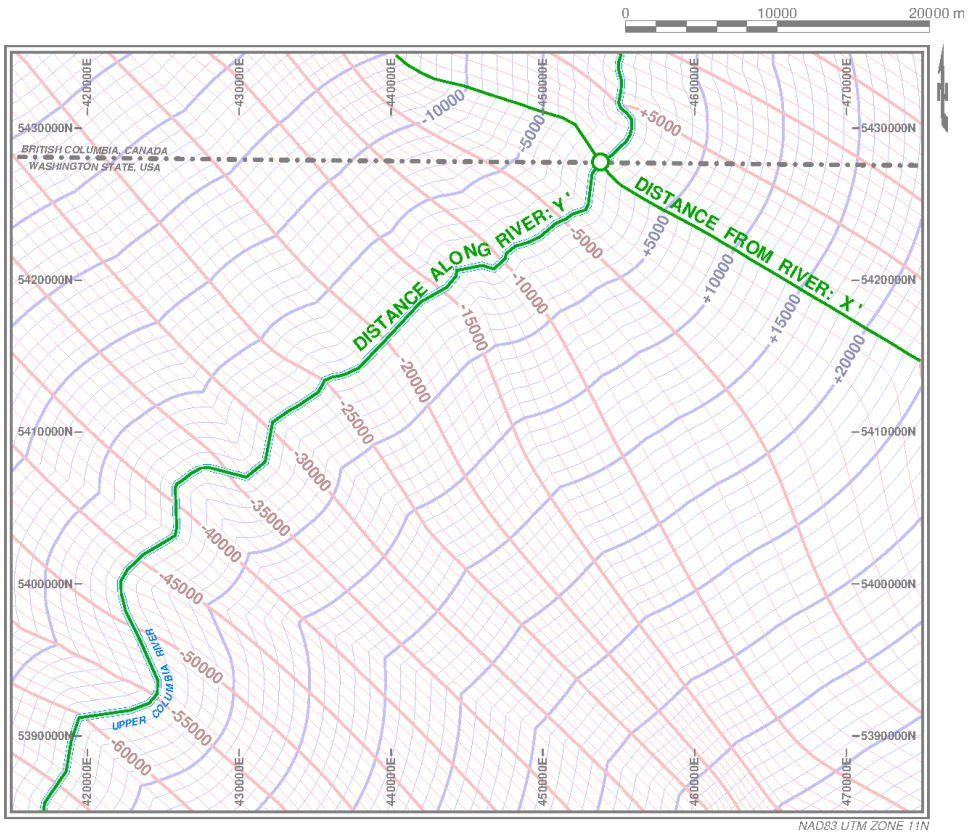

Figure 8 - Flexible grid gives local directions of maximum and minimum continuity

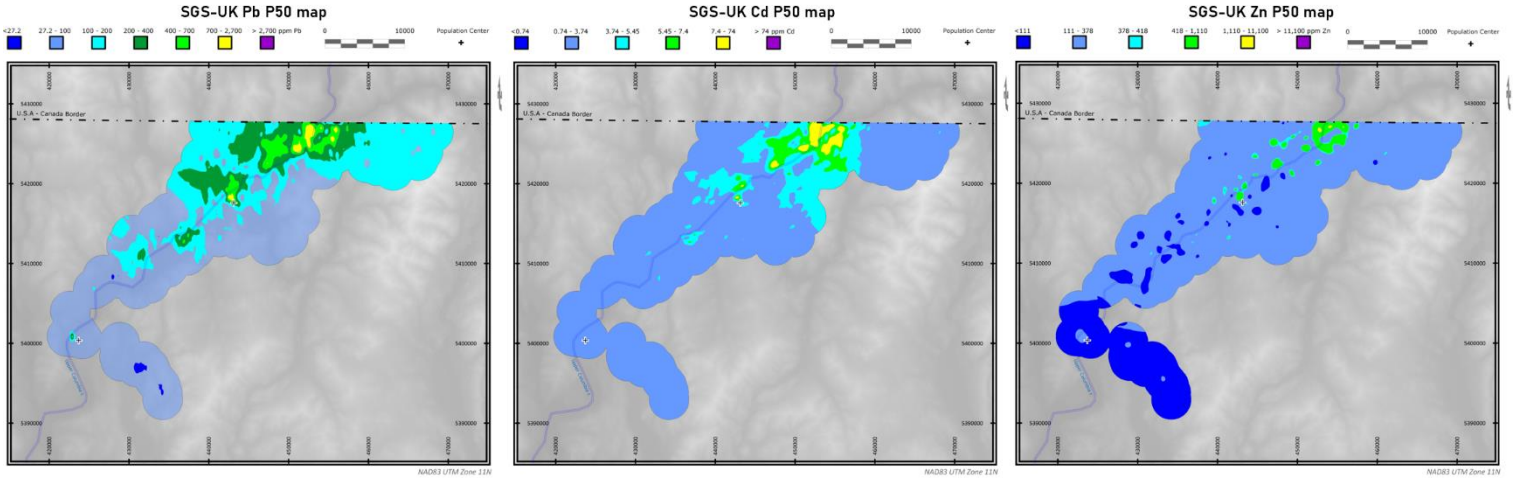

Figure 9 - Side-by-side comparison of the P50 maps for Pb, Cd and Zn

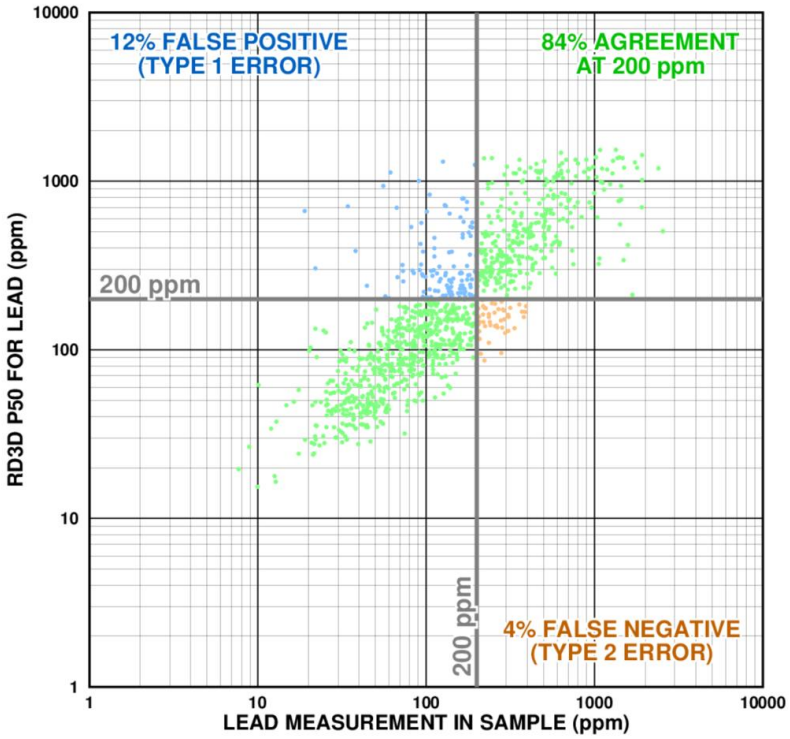

Figure 10 - Scatterplot showing the misclassification rate for Pb at 200 ppm

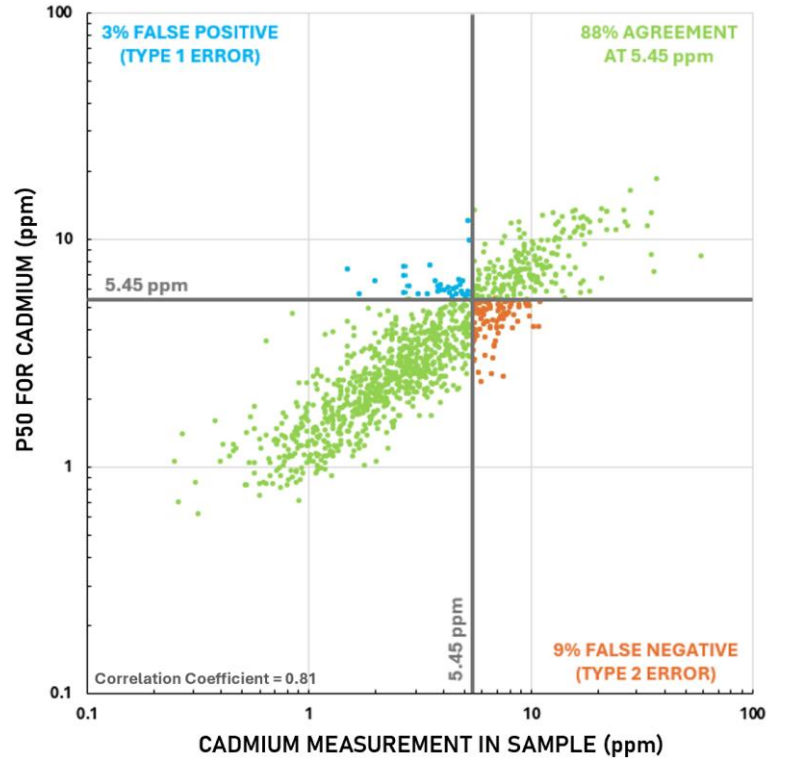

Figure 11 - Scatterplot showing the misclassification rate for Cd at 5.45 ppm

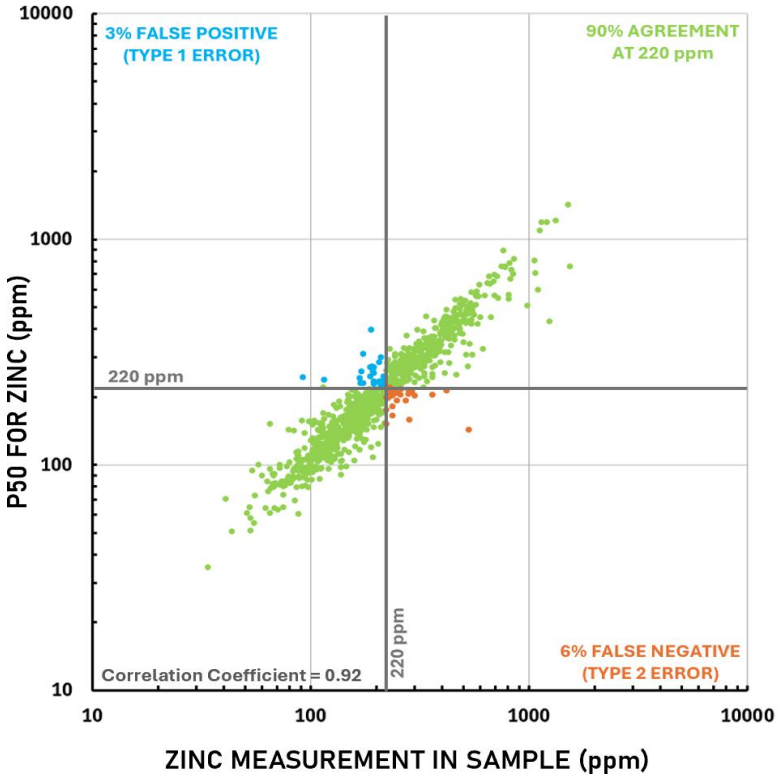

Figure 12 - Scatterplot showing the misclassification rate for Zn at 220 ppm

Tables

Table 1 - Summary statistics comparison for Pb Subset I (SUB1) and Subset II (SUB2)

	Pb (ppm) SUB1	Pb (ppm) SUB2
Number	1106	300
Mean	224.1	5709.3
Standard Deviation	295.2	20758.2
Coefficient of Variation	1.3	3.6
Max	2840	181000.0
75th Percentile	265.8	2115.0
Median	126	102.5
25th Percentile	62.4	17.0
Min	7.7	2.6

Table 2 - Summary statistics comparison for Cd Subset I (SUB1) and Subset II (SUB2)

	Cd (ppm) SUB1	Cd (ppm) SUB2
Number	1106	300
Mean	4.5	41.5
Standard Deviation	4.8	119.4
Coefficient of Variation	1.1	2.9
Max	59.3	1090.0
75th Percentile	5.7	23.5
Median	3.0	3.7
25th Percentile	1.7	0.6
Min	0.3	0.0

Table 3 - Summary statistics comparison for Zn Subset I (SUB1) and Subset II (SUB2)

	Zn (ppm) SUB1	Zn (ppm) SUB2
Number	875	300
Mean	285.4	10806.7
Standard Deviation	1251.5	34854.2
Coefficient of Variation	4.4	3.2
Max	36900	431000.0
75th Percentile	295.5	6612.5
Median	192.0	893.5
25th Percentile	129.5	90.8
Min	23.5	8.1

Table 4 - Summary of parameters used for each element

Parameter	Lead	Cadmium	Zinc
p for Box-Cox Transf.	-0.1	0.0	0.0
Relative Nugget Effect	0.55	0.5	0.4
Model Shape	Spherical	Spherical	Spherical
Range (Distance along River)	1500	1500	1500
Range (Distance from River)	500	500	500

Table 5 - Cross-validation statistics for Pb - Lab v P50

	Lab	***P50***
Number	1080	1080
Mean	140.8	126.1
Standard Deviation	146	157.9
Coefficient of Variation	1.0	1.3
Max	1537	2550
75th Percentile	166.7	152
Median	99.7	81.9
25th Percentile	54.0	38.4
Min	15.4	7.7
Correlation Coefficient	0.71	

Table 6 - Cross-validation statistics for Cd - Lab v P50

	Lab	***P50***
Number	1080	1080
Mean	4.6	3.9
Standard Deviation	4.8	2.7
Coefficient of Variation	1.1	0.7
Max	59.3	18.4
75th Percentile	5.8	5.1
Median	3.0	3.0
25th Percentile	1.7	2.0
Min	0.25	0.62
Correlation Coefficient	0.81	

Table 7 - Cross-validation statistics for Zn - Lab v P50

	Lab	***P50***
Number	849	849
Mean	243.8	231.3
Standard Deviation	175.6	146.2
Coefficient of Variation	0.7	0.6
Max	1550	1279.5
75th Percentile	297	287.4
Median	193	187.4
25th Percentile	131	136.6
Min	33.9	36.8
Correlation Coefficient	0.92	

Table 8 - Classification agreement for Pb at each threshold

Threshold (ppm Pb)	Classification Agreement (%)
27.2	97
100	83
200	84
400	89
700	92

Table 9 - False negative rate for Pb at each threshold

Threshold (ppm Pb)	False Negative Rate (%)
27.2	0
100	4
200	4
400	2
700	1

Table 10 - False positive rate for Pb at each threshold

Threshold (ppm Pb)	False Positive Rate (%)
27.2	3
100	13
200	12
400	9
700	7

Table 11 - Classification agreement for Cd at each threshold

Threshold (ppm Cd)	Classification Agreement (%)
0.74	96
3.74	87
5.45	88
7.4	90
74	100

Table 12 - False negative rate for Cd at each threshold

Threshold (ppm Cd)	False Negative Rate (%)
0.74	0
3.74	7
5.45	9
7.4	9
74	0

Table 13 - False positive rate for Cd at each threshold

Threshold (ppm Cd)	False Positive Rate (%)
0.74	3
3.74	6
5.45	4
7.4	1
74	0

Table 14 - Classification agreement for Zn at each threshold

Threshold (ppm Zn)	Classification Agreement (%)
111	91
220	90
378	95
1110	100
11100	100

Table 15 - False negative rate for Zn at each threshold

Threshold (ppm Zn)	False Negative Rate (%)
111	3
220	6
378	4
1110	0
11100	0

Table 16 - False positive rate for Zn at each threshold

Threshold (ppm Zn)	False Positive Rate (%)
111	6
220	3
378	1
1110	0
11100	0

References

(1964) G.E.P. Box and D.R. Cox, “An Analysis of Transformations,” Journal of the Royal Statistical Society: Series B (Methodological), v. 26, n. 2, p. 211-243.
(1969) G. Matheron, "Le krigeage universel (universal kriging),” Cahiers du Centre de morphologie mathématique de Fontainebleau, École nationale supérieure des mines de Paris, v. 1, 83 pages.
(1988) E. Englund and A. Sparks, “Geo-EAS (Geostatistical Environmental Assessment Software) user's guide,” EPA Environmental Systems Monitoring Lab, Las Vegas, 132 pages.
(1993) J.J. Gómez-Hernández and A.G. Journel, “Joint sequential simulation of multi-gaussian fields,” Geostatistics Tróia ’92, Kluwer Academic Publishers, v. 1, p. 85-94.